Isomeric Lifetime Measurement in the Neutron-rich ^{189}Ta

Sultan Alhomaidhi[1,2,3,4*], *Elif* Sahin[1,2,3], *Volker* Werner[1,3], *Jan* Jolie[5], *Patrick* Regan[12], *Norbert* Pietralla[1], *Jürgen* Gerl[2], *Magdalena* Górska[2], *Giovanna* Benzoni[7,8], *Andrew K.* Mistry[2], *Nicolas* Hubbard[1,2,3], *Guler* Aggez[2], *Helena M.* Albers[2], *Tugba* Arici[2], *Michael* Armstrong[2,5], *Akashrup* Banerjee[2], *Biswarup* Das[2], *Thomas* Davinson[6], *Oscar* Hall[6], *Ivan* Kojouharov[2], *Pavlos* Koseoglou[1,3], *Michal* Mikolajczuk[2,23], *Zsolt* Podolyák[12], *Marta* Polettini[7,8], *Matthias* Rudigier[1], *Henning* Schaffner[2], *Hans-Jürgen* Wollersheim[2], *Aleksandrina* Yaneva[2,5], *Plamen* Boutachkov[2], *Timo* Dickel[2], *Emma* Haettner[2], *Henning* Heggen[2], *Christine* Hornung[2], *Ronja* Knöbel[2], *Daria* Kostyleva[2], *Nikolaus* Kurz[2], *Natalia* Kuzminchuk[2], *Ivan* Mukha[2], *Stephane* Pietri[2], *Wolfgang* Plaß[2], *Christoph* Scheidenberger[2], *Yoshiki* Tanaka[2], *Helmut* Weick[2], *Usama* Ahmed[1,3], *Özge* Aktas[13], *Alejandro* Algora[14], *Corrigan* Appleton[6], *Andrey* Blazhev[5], *Alison* Bruce[10], *Bo* Cederwall[13], *Muhammad M. R.* Chishti[12,24], *Martha L.* Cortes[2], *Fabio* Crespi[7,8], *Jose J.* Dobon[18], *Maria* Doncel[20], *Aysegül* Ertoprak[13], *Arwin* Esmaylzadeh[5], *Marcos L.* Expósito[11], *Luis M.* Fraile[11], *Jaime B.* García[11], *Andrea* Gottardo[18], *Jeongsu* Ha[9], *Shaheen* Jazrawi[12], *Philipp R.* John[1], *Calum* Jones[2], *Vasil* Karayonchev[5], *Ralph* Kern[2], *Lukas* Knafla[5], *Gregor* Kosir[16,19], *Radomira* Lozeva[21], *Daniele* Mengoni[9], *Theo J.* Mertzimekis[17], *Bénédicte* Million[8], *Anabel* Morales[14], *Javier R.* Murias[11], *Sonja E. A.* Orrigo[14], *Julgen* Pellumaj[18], *Stefanos* Pelonis[17], *Jana* Petrović[13], *Sara* Pigliapoco[9], *Begoña* Quintana[22], *Francesco* Recchia[9], *Kseniia* Rezynkina[9], *Lewis* Sexton[6], *Nara* Singh[15], *Pär-Anders* Söderström[25], *Arshiya* Sood[13], *Polytimos* Vasileiou[17], *Jelena* Vesic[16], *Johannes* Wiederhold[1], *guangxin* zhang[9], *Radostina* Zidarova[1,3] and *Aikaterini* Zyriliou[17].

[1]Institut für Kernphysik, Technische Universität Darmstadt, 64289 Darmstadt, Germany
[2]GSI Helmholtzzentrum für Schwerionenforschung GmbH, 64291 Darmstadt, Germany
[3]Helmholtz Forschungsakademie Hessen für FAIR (HFHF)
[4]King Abdulaziz City for Science and Technology, P.O Box 6080, Riyadh 11442, Saudi Arabia
[5]Institut für Kernphysik, Universität zu Köln, 50937 Köln, Germany
[6]School of Physics and Astronomy, University of Edinburgh, EH9 3FD Edinburgh, UK
[7]Universita degli Studi di Milano, Via Celoria 16, 20133, Milano, Italy
[8]INFN, sez. di Milano, Via Celoria 16, 20133, Milano, Italy
[9]Dipartimento di Fisica e Astronomia dell'Universita di Padova and INFN Padova, 35131, Padova, Italy
[10]School of Computing, Engineering, and Mathematics, University of Brighton, BN2 4GJ Brighton, UK
[11]Grupo de Física Nuclear and IPARCOS, Universidad Complutense de Madrid, CEI Moncloa, E-28040 Madrid, Spain
[12]Department of Physics, University of Surrey, GU2 7XH Guildford, UK
[13]KTH Royal Institute of Technology, Stockholm, Sweden
[14]Instituto de Física Corpuscular, CSIC-Universidad de Valencia, E-46071 Valencia, Spain
[15]School of Computing, Engineering and Physical Sciences, University of the West of Scotland, PA1 2BE Paisley, UK
[16]Jozef Stefan Institute, Jamova cesta 39, 1000 Ljubljana, Slovenia
[17]National and Kapodistrian University of Athens, Athens 157 72, Greece
[18]INFN Laboratori Nazionali di Legnaro, Viale dell'Università 2, 35020 Legnaro PD, Italy
[19]Faculty of Mathematics and Physics, University of Ljubljana, Ljubljana, Slovenia
[20]Stockholm University, SE-106 91 Stockholm, Sweden
[21]Université Paris-Saclay, IJCLab, CNRS/IN2P3, F-91405 Orsay, France
[22]Universidad de Salamanca, 37008 Salamanca, Spain
[23]Faculty of Physics, University of Warsaw, 00-681 Warsaw, Poland
[24]Department of Physics, Lund University, SE-221 00 Lund, Sweden
[25]Extreme Light Infrastructure-Nuclear Physics (ELI-NP)/Horia Hulubei National Institute for Physics and Nuclear Engineering (IFIN-HH), Str. Reactorului 30, Magurele 077125, Romania

Abstract. Isomeric states of the neutron-rich isotope $^{189}_{73}\mathrm{Ta}_{116}$ were populated via fragmentation of a primary beam of ^{208}Pb ions at 1 GeV/u impinging on a ^{9}Be target at GSI, Darmstadt, Germany. The isotopes of interest were separated, identified and delivered to the DESPEC setup. Two isomers were deduced in $^{189}\mathrm{Ta}_{116}$ and their lifetimes were measured based on the γ-ray time distributions.

1 Introduction

Neutron-rich nuclei in the A ~ 190 mass region exhibit a variety of nuclear structural properties. For instance, well deformed prolate, triaxial, oblate and spherical shapes (at N = 126) could be characterized by the properties of their respective ground-state shapes [1-4]. The evolution from prolate to oblate nuclei passing

* Corresponding author: s.alhomaidhi@gsi.de

through the γ-soft nuclei have been described as the prolate-oblate phase transitional systems [5]. In odd-mass systems, the shape of the atomic nucleus is influenced by the addition of an unpaired particle or hole. A study of odd-A neutron-rich Rhenium isotopes (Z =75) in the A ~ 190 region indicated increasing γ deformation and the evolution of triaxiality with increasing neutron number [6]. The $^{187}Ta_{114}$ nucleus was studied recently using multinucleon transfer (MNT) reactions by Walker et al. The γ rays depopulating the isomeric states of $^{187}Ta_{114}$ were associated with a perturbed rotational band, showing the prolate-oblate shape transition effect [7].

However, with increasing neutron number, it becomes difficult to synthesize and select isotopes using MNT reactions and the isotope separation method. To overcome this obstacle, projectile fragmentation reactions at relativistic energies proved to be an efficient method for populating states in neutron-rich isotopes. For $^{189}Ta_{116}$, two data sets were obtained from the RISING campaigns in 2006 and 2007, which reported different isomeric half-lives of $T_{1/2}$ = 1.6(2) μs [8] and $T_{1/2}$ = 0.58(22) μs [9], respectively. The involvement of two different isomeric states were assumed to explain the discrepancy in half-lives.

The $^{189}Ta_{116}$ nucleus and other neutron-rich nuclei in the A~190 region were populated for the study of shape evolution, using the projectile fragmentation reactions at GSI Helmholtzzentrum für Schwerionenforschung. The spectroscopic study was carried out using the DEcay SPECtroscopy (DESPEC) [10] setup within the FAIR Phase-0 campaign in March 2021.

2 Experimental Details

The nuclei of interest were produced by the fragmentation of a 1 GeV/u primary beam of ^{208}Pb, impinging on a 2.7 g/cm^2 ^{9}Be target. The primary beam was delivered by the UNILAC and SIS-18 synchrotron with a beam intensity of up to 10^9 ions/s. The fragments were separated and identified on an event-by-event basis in the FRagment Separator (FRS) [11], operated in the standard achromatic mode with an Al degrader placed in its intermediate focal plane. The FRS was tuned to transmit fully-stripped $^{190}Ta_{117}$ ions in the central trajectory of the FRS to the final focal plane. A summary of the FRS setting is shown in Table 1.

Table 1. Summary of FRS setting parameters.

Parameter	Value
Magnetic rigidity $B\rho_{12}$	12.5166 Tm
Magnetic rigidity $B\rho_{34}$	10.5367 Tm
S2 degrader thickness	2500 mg/cm^2
S4 degrader thickness	4838 mg/cm^2
Spill length	1.5 s

A series of detectors at the intermediate and final focal planes of the FRS were used for the secondary beam identification. The time of flight (ToF) was determined by measuring the time difference between the two scintillation detectors placed at the intermediate and the final focal planes of the FRS. Time projection chambers (TPCs) were used for position measurements. Two multi-sampling ionization chambers (MUSICs), placed at the final focal plane, were used for the energy loss (ΔE) measurements.

An Al degrader was used to decelerate the ions arriving at the final focal plane and allowed for their implantation into an active stopper, the Advanced Implantation Detector Array (AIDA) [12]. AIDA consisted of 3 layers of (8 x 8) cm^2 Double-Sided Silicon Strip Detectors (DSSSDs), for the identification of the implanted ions and the subsequent β decays. Two fast plastic scintillators were mounted upstream and downstream of AIDA with 10 mm distance for the β-decay timing. The downstream plastic was also used for vetoing light ions passing through the detectors. Surrounding AIDA, two high-purity Ge cluster detectors of the EUROBALL array [13], each with 7 segments, and 36 $LaBr_3$(Ce) detectors of the FAst TIMing Array (FATIMA) [14] were used to detect γ radiation. The $LaBr_3$(Ce) detectors were used for fast-timing spectroscopy, while HPGe detectors provided precise energy information.

All the subsystems of the DESPEC setup were triggered independently, in which the White Rabbit common time clock with ~ 1 ns precision was employed to correlate the events (for more details about the setup, the reader is referred to Ref. [10]).

3 Analysis and Results

As the particle identification is based on the mass-over-charge ratio (A/Q) as a function of the atomic number (Z), the charge states of the ions traversing the FRS must be selected first. Previous studies in the A ~ 190 mass region have shown how the different charge states can overlap in the particle ID plot [8, 9]. In particular, isotopes with atomic mass equal to (A – 3), Z and charge (Q = Z – 1), have comparable magnetic rigidity to fully-stripped ions (A, Q = Z). Fully-stripped ions transmitted through the FRS can pick up an electron when they interact with matter and detectors at the intermediate focal plane. In order to overcome this, the energy loss ΔE_{deg} in the degrader in the intermediate focal plane can be deduced from the difference in the magnetic rigidity, Bρ, between the first and the second halves of the FRS. The charge states of the ions were determined by correlating the energy loss, ΔE_{deg}, with the atomic number (Z) [15].

As shown in Fig. 1, two main isotopic regions (1, 2) in the two-dimensional plot can be seen, one is for the H-like ions from Platinum (Z = 78) to Osmium (Z = 76), and the second region corresponds to the fully-stripped ions from Rhenium (Z = 75) to Hafnium (Z = 72). The isotopes from Z = 76 to 78 acquire an electron at the mid-focal plane and retain it to the final focal plane.

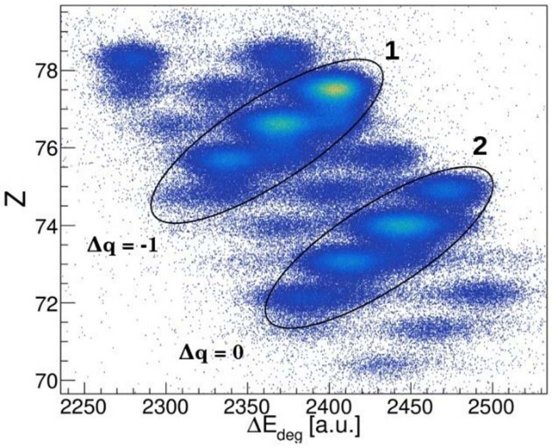

Fig. 1. (color online) Two-dimensional plot of the effective energy loss ΔE_{deg} as function of Z. Region (1): H-like charge state ions from (Z = 78 to 76). Region (2): fully-stripped ions from (Z = 75 to 72).

After the particle identification, the fully-stripped ions (Q = Z), shown in Fig. 2, were used for the γ-spectroscopic analysis. The presence of the delayed 292 keV γ-ray transition in the $^{188}Ta_{115}$ isotope [16], confirms the validity of the used method.

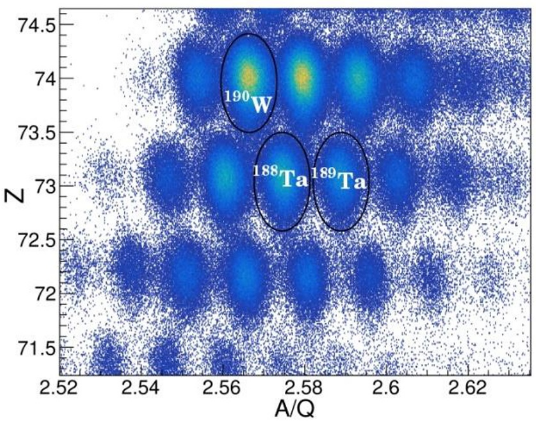

Fig. 2. (color online) Particle identification plot. The main isotopes of interest in the experiment are labelled (^{190}W, ^{188}Ta, ^{189}Ta).

The γ rays decaying from the isomeric states in ^{189}Ta were detected within a time widow of 10 μs for HPGe clusters and 7 μs for the LaBr₃(Ce) detectors after the implantation. The presence of previously-reported 83, 134, 154, 199, 246, 283, 389 and 481 keV γ-ray transitions have been confirmed in the present data set. As shown in Fig. 3, the delayed γ-ray transitions spectrum, where the energy peaks are labelled, as recorded in HPGe detectors.

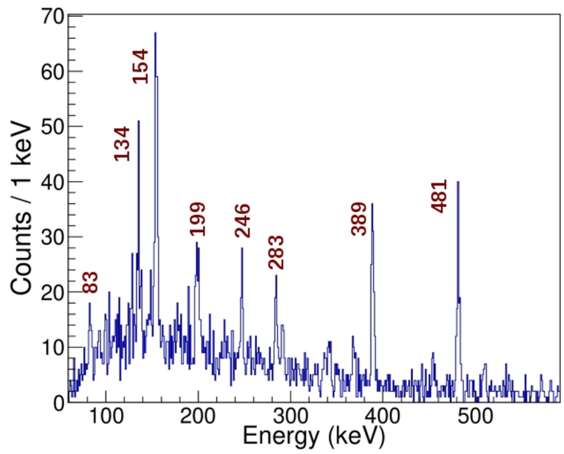

Fig. 3. Delayed energy spectrum of the γ rays known in ^{189}Ta as registered in HPGe detectors.

In the previous measurements by Alkhomashi et al. and Steer et al., one isomeric state was identified. The half-life of the isomer was reported to be $T_{1/2}$ = 1.6(2) μs and $T_{1/2}$ = 0.58(22) μs in [8] and [9], respectively. In this experiment, two isomeric states have been identified. The γ-ray emission time was registered with respect to the time of implantation. The time behaviour of the 134 keV transition, as shown in Fig. 4, shows a shorter decay constant in comparison with time behaviour of the 154, 283, 389 and 481 keV transitions.

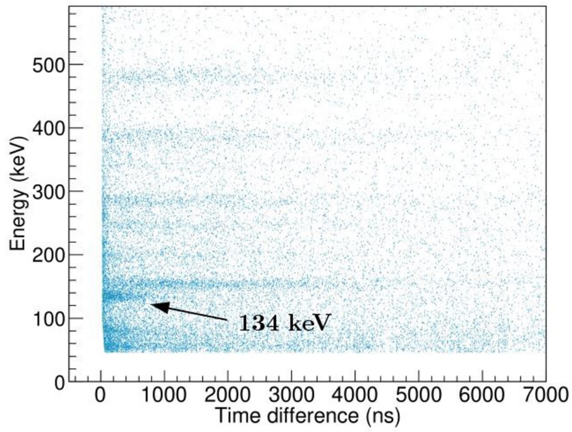

Fig. 4. (color online) The energy-time matrix for the $LaBr_3$(Ce) detectors. The 134 keV γ-ray transition is indicated by the black arrow.

The 154, 199, 246, 283, 389 and 481 keV γ-ray transitions were found to be in coincidence within a ~ 10 ns time window of the γ-γ-ΔT cube. The 134 keV transition is in coincidence with the other transitions mentioned above, when the ΔT range is long (10 ns < ΔT < 5 μs). The time difference between transitions for example: ΔT (154 keV – 134 keV) > 10 ns suggests that the first isomer is decaying from a higher-lying energy state via a 134 keV γ-ray, feeding the second isomer which then depopulates to the ground state via other γ-ray transitions.

With a single-component exponential decay fit to the time difference distribution of the 134 keV transition with respect to the implant time, the half-life of the first isomer was estimated to be $T_{1/2}$ ~ 200 ns. For the second isomer, fitting to the exponential decay of the sum of the time difference distributions of the 154, 283, 389 and 481 keV γ-ray transitions yields a half-life of $T_{1/2} \sim 1.2$ μs. A comparison with theoretical calculations, interpretation of the isomeric states and a suggestion for the level scheme for the neutron-rich $^{189}Ta_{116}$ isotope will be reported elsewhere [17].

4 Conclusions

The isomeric states of $^{189}Ta_{116}$ were produced by fragmentation reactions at the GSI accelerator facility, Darmstadt. The study of γ rays via spectroscopy using the DESPEC setup shows that two isomers are present in this isotope. The half-life of the shorter isomer was estimated to be $T_{1/2} \sim 200$ ns, and $T_{1/2} \sim 1.2$ μs for the longer one. The γ-γ-ΔT analysis has shown that the shorter isomer is decaying from a higher-lying energy state and feeding the second isomer.

The authors would like to thank the staff of the FRS and the GSI accelerator for their support. The results were obtained in the context of FAIR Phase-0 Darmstadt, Germany. This work was supported by BMBF under Verbundprojekt 05P2021 (ErUM-FSPT07) grants 05P21PKFN1 and 05P21RDFN1; by STFC(UK); by the Helmholtz Research Academy Hesse for FAIR (HFHF). PAS was supported by contract PN 23.21.01.06 sponsored by the Romanian Ministry of Research, Innovation and Digitalization. S.A. acknowledges support from King Abdulaziz City for Science and Technology for the Ph.D. funding.

References

1. R. F. Casten, Nucl. Phys. **A443**, 1 (1985).
2. P. D. Stevenson, M. P. Brine, Z. Podolyak, P. H. Regan, P. M. Walker, and J. R. Stone, Phys. Rev. C **72**, 047303 (2005).
3. P. Sarriguren, R. Rodriguez-Guzman, and L. M. Robledo, Phys. Rev. C **77**, 064322 (2008).
4. L. M. Robledo, R. Rodríguez-Guzmán, and P. Sarriguren, J. Phys. G: Nucl. Part. Phys. **36**, 115104 (2009).
5. J. Jolie and A. Linnemann, Phys. Rev. C **68**, 031301(R) (2003).
6. M. W. Reed, et al., Phys. Lett. B **752**, 311 (2016).
7. P. M. Walker, et al., Phys. Rev. Lett. **125**, 192505 (2020).
8. N. Alkhomashi, et al., Phys. Rev. C **80**, 064308 (2009).
9. S. J. Steer, et al., Phys. Rev. C **84**, 044313 (2011).
10. A.K. Mistry et al., Nucl. Instrum. Meth. Phys. Res. A **1033** (2022) 166662.
11. H. Geissel et al., Nucl. Instrum. Methods Phys. Res., Sect. B **70**, 286 (1992).
12. Available: https://edms.cern.ch/ui/file/1865809/2/TDR_HISPEC_DESPEC_AIDA_public.pdf
13. J. Simpson, The Euroball Spectrometer, Z. Phys. A **358** (1997).
14. M. Rudigier et al., Nucl. Instrum. Methods Phys. Res. A **969**, 163967 (2020).
15. J. Benlliure,K.-H. Schmidt,D.Cortina-Gil, T. Enqvist, F. Farget, A. Heinz, A. R. Junghans, J. Pereira, and J. Taieb, Nucl. Phys. A**660**, 87 (1997).
16. M. Caamaño et al., Eur. Phys. J. A **23**, 201 (2005).
17. S. Alhomaidhi et al., (to be published).